DEVELOPMENT OF POLYSACCHARIDE-CASEIN GEL-LIKE STRUCTURES RESISTANT TO *IN VITRO* GASTRIC DIGESTION

Cynthia Fontes-Candia[1], Pablo Jiménez-Barrios[2], Beatriz Miralles[2], Isidra Recio[2], Amparo López-Rubio[1], Marta Martínez-Sanz[2*]

[1]Food Safety and Preservation Department, IATA-CSIC, Avda. Agustín Escardino 7, 46980 Paterna, Valencia, Spain

[2]Instituto de Investigación en Ciencias de la Alimentación, CIAL (CSIC-UAM, CEI UAM + CSIC), Nicolás Cabrera, 9, 28049 Madrid, Spain

*Corresponding author: Tel.: +34 910017817

E-mail address: marta.martinez@csic.es

Abstract

Controlling protein digestion is a promising strategy to modulate hormonal responses involved in satiety and appetite regulation. In this context, polysaccharide-casein gel-like structures have been developed and subjected to *in-vitro* gastrointestinal digestions to evaluate their potential for delaying casein hydrolysis. The effect of the polysaccharide type (agar vs. κ-carrageenan), the polysaccharide:casein ratio and the physical state of the structures (hydrogels *vs*. aerogels) on the protection ability was investigated. The microstructure evolution of the materials upon the digestions was studied and the molecular weight distribution and peptidomic profile of the digestion products were also determined.

During the gastric phase most of the developed structures exerted a protective effect and intact casein clusters were even detected in some of the formulations. In contrast, during the intestinal phase most of the casein was released and hydrolysed to a certain extent. In general, the hydrogels showed a greater protective effect than the aerogels, due to a limited diffusion of the protein towards the liquid medium. Moreover, a higher polysaccharide:protein ratio produced stronger gel networks which provided greater protection. In particular, agar-based and κ-carrageenan hydrogels with 25% polysaccharide and agar-based aerogels with 75% polysaccharide would be the most optimum for delaying casein digestion, since they were able to preserve intact casein after the gastric phase while promoting the release of peptides during the intestinal phase.

Keywords: Controlled digestibility, simulated gastrointestinal digestion, sulphated polysaccharides, aerogels, hydrogels

1. Introduction

During the gastrointestinal digestion process, food undergoes physical, chemical and biochemical changes that promote the release of nutrients, which will be further used by the organism. Proteins are known to be extensively hydrolysed throughout the digestive tract by the gastrointestinal environment, leading to the release of numerous peptides and free amino acids. In the stomach, proteins are digested by pepsin, while in the small intestine they are hydrolysed by the action of several pancreatic proteases. Amongst milk proteins, globular and compact proteins like β-lactoglobulin are resistant to the action of pepsin, while other proteins with a looser structure like caseins are hydrolysed into smaller polypeptides by the action of this enzyme (Apong, 2019). The micellar structure of casein is readily disassembled upon gastric digestion, followed by clotting, and producing a complex mixture of peptides and free amino acids (Miralles et al., 2021). Protein digestibility does not only determine the bioavailability of essential units with nutritional value, but may also cause changes along the gastrointestinal tract, such as metabolic and immune responses, epithelial and microbial changes (Dallas et al., 2017). In fact, some peptides generated upon protein digestion are able to interact with different receptors expressed on the surface of enteroendocrine cells in the gut, which in turn, secrete hormones controlling the digestive process and regulating food intake (Caron et al., 2016). In this context, protein digestion could be controlled throughout technological treatments, such as heat treatments or cross-linking, with the aim of causing different metabolic responses. For instance, casein cross-linking has been shown to induce a more sustained release of hormones such as cholecystokinin (CCK) and a stronger feeling of fullness than control casein or whey, suggesting that food structure can modulate postprandial

responses (Juvonen et al., 2011). As an alternative, the encapsulation of proteins using gastric resistant matrices is a promising approach to generate protein-rich products with the potential to induce a higher release of anorexigenic hormones or to protect protein compounds to be delivered in distal intestinal regions. Although methods such as atomization (Putney, 1998) and electrohydrodynamic processing (Xiaoqiang Li et al., 2010; Xie & Wang, 2007) have been used for the encapsulation and protection of proteins, these technological processes may require denaturation of the proteins to get them fully solubilized or induce denaturation upon processing and thus, other methods such as gelation may be preferred for food-related applications. In this sense, exploiting the ability of proteins to form complexes with polysaccharides is an efficient strategy to produce hybrid gels that may exert a protective effect on the proteins (Alavi et al., 2018).

Many works have reported the formation of protein-polysaccharide hybrid gel networks where the protein has been denatured to induce its capacity to form gels (de Jong, Klok, & van de Velde, 2009; Xianghong Li, Hua, Qiu, Yang, & Cui, 2008; Zhang, Zhang, & McClements, 2017; Zhang, Zhang, Zou, & McClements, 2016), while fewer works have focused on the incorporation of native proteins within the network of a gelling polysaccharide. Alginate and chitosan are the most widely used polysaccharides to encapsulate proteins or peptides through gelation and to delivery systems (Gombotz & Wee, 2012; Ozel, Zhang, He, & McClements, 2020; Zhang et al., 2016). However, chitosan-based hydrogels are pH-dependent and swell at acidic pH, which could lead to the undesired release of protein in the stomach (Yuan, Jacquier, & O'Riordan, 2018). Sulphated polysaccharides such as agar and κ-

carrageenan are able to form hydrogels with a varied range of mechanical and structural properties (Fontes-Candia, Ström, Gómez-Mascaraque, López-Rubio, & Martínez-Sanz, 2020; Martínez-Sanz et al., 2020), being an alternative to design encapsulation matrices oriented to protect protein structures during gastrointestinal conditions. Furthermore, these gels can be subjected to drying processes, yielding porous structures known as aerogels (Agostinho et al., 2020; Manzocco et al., 2017), with potential as controlled delivery systems.

In terms of protein digestibility, interactions between proteins and polysaccharides have been studied as the latter are well known to impart different viscoelastic properties which have an impact on the digestion process. Moreover, the physical structure of the materials also will influence the protein digestion. Markussen et al. described the influence of different hydrocolloids such as alginate, pectin and guar gum on the digestibility of milk proteins, concluding that the presence of polysaccharides has a significant impact on gastric emptying and protein digestion kinetics (Markussen, Madsen, Young, & Corredig, 2021). Furthermore, the electrostatic complexation of proteins to polysaccharides may limit their susceptibility to the hydrolytic action of digestive enzymes (Mouécoucou, Villaume, Sanchez, & Méjean, 2004). Recent works have reported on the complexation of soy, pea and whey proteins with k-carrageenan (Ozel et al., 2020), and whey protein isolate with alginate (Zhang et al., 2017), resulting in a higher resistance to gastric conditions in comparison with control proteins, which might be useful to modulate hormonal responses and appetite. Another important aspect to consider is that the incorporation of these

protein-polysaccharide complexes into different types of food matrices is expected to have a strong impact on their digestibility and, thus, this should be studied in the future.

Based on this, we aimed to develop hybrid polysaccharide-casein gel-like structures capable of shifting protein digestion towards the intestine. Casein was chosen as a model protein due to its high susceptibility to hydrolysis upon gastric digestion. The influence of the polysaccharide type (agar vs. κ-carrageenan) and the physical state of the gel-like structures (hydrated hydrogels vs. freeze-dried aerogels) on the ability to protect casein upon *in vitro* gastric digestion were evaluated and the generated digestion products were characterized in terms of microstructure, molecular weight distribution and peptidomic analyses. Understanding the digestion mechanism on the developed structures will open up the possibility of designing novel dietary products to modulate postprandial response and satiety.

2. Materials and methods

2.1. Materials

Commercial κ-carrageenan (Ceamgel 90-093) and agar (PRONAGAR), in the form of powders, were kindly donated by CEAMSA (Pontevedra, Spain) and Hispanagar (Burgos, Spain), respectively. The commercial κ-carrageenan grade was composed of 92% κ-carrageenan and 8% ι-carrageenan (Fontes-Candia, Ström, Gómez-Mascaraque, et al., 2020). The agar content in the commercial agar was 80% (Martínez-Sanz et al., 2020). Casein powder in the form of micellar casein (with a protein content of 78.4%) was supplied by Ingredia (Arras, France). KCl was purchased from Sigma-Aldrich (Spain).

144

145 **2.2. Preparation of polysaccharide-casein gel-like structures**

146 Polysaccharide-casein gel-like structures were produced by using κ-carrageenan and
147 agar as the gelling matrices (coded as KC and A, respectively). After gelation of the
148 polysaccharides, the materials were used in their hydrated state, i.e., hydrogels (coded
149 as HG) and after being subjected to a freeze-drying process to remove water and obtain
150 porous dry materials known as aerogels (coded as AG). Firstly, polysaccharide and
151 casein solutions in water were prepared separately. To obtain hydrogels with good
152 mechanical integrity, the concentration of the polysaccharide and casein solutions was
153 fixed at 2% (w/v), based on previous experiments (Fontes-Candia, Ström, López-
154 Sánchez, et al., 2020; Martínez-Sanz et al., 2020). The casein and polysaccharide
155 powders were dispersed in hot water (at a temperature of 40 °C for the casein and 90
156 °C for the polysaccharides) for 30 min. For the κ-carrageenan samples, KCl (0.25%
157 (w/v) with respect to the carrageenan solution) was then added to the hot solution,
158 which was gently stirred until the salt was completely dissolved. The required volume
159 of casein solution was added to the polysaccharide solution and the samples were
160 homogenized by further stirring. The polysaccharide:casein ratio was set at 75:25 or
161 25:75, w/w. It should be noted that the 75:25 ratio corresponded to the maximum
162 casein content which could be incorporated into the hydrogels without compromising
163 their mechanical integrity. 0.4 mL of the polysaccharide-casein blends were
164 transferred to a cylindrical silicon mould (7 mm diameter, 10 mm height) and were
165 cooled down to room temperature and subsequently stored at 4 °C overnight. The
166 hydrogels were stored in the fridge for a maximum of 48 h prior to the *in-vitro*
167 digestions. For the preparation of the polysaccharide-casein aerogels (AG), the

prepared hydrogel samples were frozen at -80 °C and subsequently, freeze-dried using a Genesis 35-EL freeze-dryer (Virtis, Spain). The produced aerogels were stored at 0% RH. Table 1 summarizes the different formulations prepared and their corresponding sample codes.

Table 1. Composition of polysaccharide-casein gel-like structures.

Sample code	Polysaccharide type	Physical state	Polysaccharide (% w/w)	Casein (% w/w)
HG-A25	Agar	Hydrogel	25	75
HG-A75	Agar	Hydrogel	75	25
AG-A25	Agar	Aerogel	25	75
AG-A75	Agar	Aerogel	75	25
HG-KC25	κ-carrageenan	Hydrogel	25	75
HG-KC75	κ-carrageenan	Hydrogel	75	25
AG-KC25	κ-carrageenan	Aerogel	25	75
AG-KC75	κ-carrageenan	Aerogel	75	25

2.3. *In-vitro* simulated gastrointestinal digestions

The prepared hydrogel and aerogel samples were digested according to the INFOGEST *in-vitro* gastrointestinal digestion protocol (Brodkorb et al., 2019) with minor modifications. Briefly, the required amount of sample to provide 75 mg of casein was added to a polypropylene tube, 5 mL of human salivary fluid were incorporated and the sample was incubated for 5 min. Subsequently, 5 mL of simulated gastric fluid (SGF) (pH=3) containing pepsin from porcine gastric mucosa (final

pepsin concentration 2000 U/mL of gastric digest, Sigma-Aldrich, St Louis, MO, USA) were added. Gastric digestion was stopped at 120 min by adjusting the pH to 7 with 1 M NaOH. The intestinal phase was conducted by mixing the end point from the gastric phase with 10 mL of simulated intestinal fluid (SIF) (pH=7) containing pancreatin from porcine pancreas (100 U trypsin activity per mL of final mixture, Sigma-Aldrich) and porcine bile extract (Sigma-Aldrich). Since the digests will be tested in cell lines in future works, the bile salt concentration was reduced to 2.5 mM, given the cytotoxic effects of 10 mM bile salts in the STC-1 cell line reported by (Santos-Hernández, Tomé, Gaudichon, & Recio, 2018). The intestinal digestion was stopped after 120 min by heating the sample at 85 °C for 15 min. In most of the cases, the gastric and intestinal digests could be separated into two phases: a solid fraction consisting of the non-digested material and the liquid fraction containing the digested soluble compounds. These two phases were separately characterized for each formulation after each digestion step, giving rise to four different samples: gastric solid (GS), gastric liquid (GL), intestinal solid (IS) and intestinal liquid (IL). After separating the two phases, the samples were subjected to snap freezing in liquid nitrogen, freeze-dried and stored at −20 °C until further analyses. Micellar casein (coded as Cas) was also subjected to the same digestion protocol and its digestion products were analysed. Finally, to evaluate the effect of the physical structures formed upon gelation, control samples were prepared by physically blending the casein with the polysaccharides prior to the digestion (i.e., without subjecting the polysaccharides to the gelation process). The polysaccharide:protein ratios were the same used for the hydrogels and aerogels, i.e., 75:25 and 25:75. These control samples were coded as C-A75 and C-A25 in the case of the agar formulations and C-KC75 and C-KC25 for the

κ-carrageenan formulations. For each specific formulation the digestions were performed in triplicate by using individual tubes per time point (gastric and intestinal). The nitrogen content in the freeze-dried digests was determined by elemental analysis using the Dumas method in a LECO CHNS-932 (Thermo Fisher, USA) analyser. Further analyses were performed on a protein basis according to the results.

2.4. Scanning electron microscopy (SEM)

Aerogel samples were coated with a gold-palladium mixture under vacuum and their morphology was studied using a Hitachi microscope (Hitachi S-4800) at an accelerating voltage of 10 kV and a working distance of 8–16 mm.

2.5. Confocal laser scanning microscopy (CLSM)

CLSM was used to visualize the microstructure of the polysaccharide-casein hydrogels and aerogels before and after being subjected to gastrointestinal digestion. Imaging was performed using a Confocal Microscope Leica TCS SP5 (Leica Microsystems, Germany) equipped with the LAS-AF software. Thick sections were carefully cut from solid samples with the help of a scalpel. Then, a sufficient amount of Fast Green solution (0.1% wt. in water) was added to completely soak the sample and stain the protein. After that, the sample was placed onto a microscopy glass slide and covered with a glass cover slip. The light source used was a HeNe laser with an emission wavelength of 647 nm. A lens with a magnification of 20 and a numerical aperture (NA) of 0.7 was used throughout the study. Images were processed using the Fiji software.

2.6. Sorption capacity of aerogels

The capacity of the aerogels to sorb SGF was tested by soaking the samples previously weighed into 15 mL of SGF in sealed containers. The samples were periodically taken out of the liquid and weighed using an analytical balance (Mettler-Toledo, Ms105du, Switzerland, d=0.01 mg) after removing the excess liquid. Measurements were taken until the samples were equilibrated and the total weight gain was calculated.

2.7. Gel strength

Gel strength values were determined from penetration assays, according to the method described by Marciani et al. (2019), with slight modifications. A texture analyser (Stable Micro Systems model TA-XT2, Surrey, UK) equipped with a cylindrical aluminum plunger (3.6 cm diameter) and a load cell of 30N was used. The assays were carried out at room temperature (20–25 °C). Gel disks were compressed to 80 % of the original height, using a crosshead speed of 0.1 mm/s. All measurements were performed, at least, in triplicate.

2.8. Sodium Dodecyl Sulphate-Polyacrylamide Gel Electrophoresis (SDS-PAGE)

SDS-PAGE was performed as previously described by (Santos-Hernández et al., 2018) with minor modifications. Gastric and intestinal digests were dissolved in sample buffer which contained Tris-HCl (0.05M, pH 6.8, SDS (1.6% w:v), glycerol (8% v:v), β-mercaptoethanol (2% v:v) and bromophenol blue indicator (0.002% w:v) at a protein concentration of 1.5 mg/mL and 2.0 mg/mL, respectively. The samples were heated at 95 ºC for 5 min and kept warm until they were loaded on the 12% Bis-Trispolyacrilamide gels (Criterion XT, Bio-Rad, Richmond, CA, USA).

Electrophoretic separations were carried out at 150 V using XT-MES as running buffer (Bio-Rad), in the Criterion cell (Bio-Rad). The gels were stained with Coomassie Blue (Instant Blue, Expedeon, Swavesey, UK) and images were taken with a Molecular Imager VersaDoc™ MP 5000 system (Bio-Rad, Hercules, CA, USA).

2.9. Molecular weight distribution of peptides by MALDI-TOF/TOF

Intestinal digests were reconstituted at 0.1 mg of protein/mL in 33% acetonitrile with 0.1% trifluoroacetic acid prior to being spotted into a MALDI target plate with a 2,5-dihydroxybenzoic acid matrix. Analyses were performed on an Autoflex SpeedTM (Bruker Daltonic, Bremen, Germany). Ions were detected in positive linear mode at a mass range of *m*/z 5–20 kDa for proteins and in reflectron mode at a mass range of *m*/z 500–3000 Da for peptides and were collected from the sum of 1,000 on average lasers shots. Protein Calibration Standard I and Peptide Calibration Standard, Bruker Daltonics were employed for external calibration of spectra. The monoisotopic peaks were generated using FlexAnalysis 3.3 software and were represented in a molecular weight distribution range.

2.10. Peptide identification by HPLC-tandem mass spectrometry (HPLC-MS/MS) analysis

The identification of resistant peptides to intestinal digestion was performed by HPLC-tandem mass spectrometry (HPLC-MS/MS) according (Santos-Hernández et al., 2018). Freeze-dried intestinal and gastric digests were reconstituted in solvent A (water:formic acid, 100:0.1, v:v); prior to analysis, fractions were centrifuged at

11,000 × *g* for 10 min. The spectra were recorded over the mass/charge (*m/z*) ranges of 100–600, 100–1700, and 100–2000, selecting 500, 750, and 1200 and as target mass, respectively. A homemade database of bovine casein protein was used for peptide sequencing in MASCOT v2.4 software (Matrix Science). Biotools version 3.2 was used for interpreting the matched MS/MS spectra.

2.11. Statistics

All data have been represented as the average ± standard deviation. Different letters show significant differences both in tables and graphs ($p \leq 0.05$). Analysis of variance (ANOVA) followed by a Tukey-test were used to determine significant differences between the formulation using the statistical software IBM SPSS (v.24) (IBM corp., USA).

3. Results and discussion

3.1. Structural behaviour of the polysaccharide-casein gel-like structures upon gastrointestinal digestion

While the gastric and intestinal digests from the casein and the control polysaccharide-casein blends were homogeneous, the digests from the gel-like structures were heterogeneous, presenting two different phases which were separated and analysed individually: a solid fraction (presumably containing non-digested material) and a liquid fraction composed of the digested soluble compounds. The presence of the solid phase was not surprising, since the polysaccharide gel-like structures were expected to be resistant to the digestion conditions (McClements, 2017). As an example, Figure 1 shows the visual appearance of the gel-like structures with a polysaccharide:protein

ratio of 75:25 in their initial state and the solid phases obtained after the gastric (coded as GS) and intestinal (coded as IS) digestions. As observed, the hydrogel structure for both polysaccharides remained apparently intact after the gastric and intestinal digestions. A slight change in the colouration from the hydrogels, which turned from whitish to yellowish, was noted after the intestinal digestion. This suggests that the hydrogels were able to retain a certain fraction of the bile salts (responsible for that yellowish coloration) present in the intestinal fluid within their structure. Moreover, a change in the transparency of the gels was noted after the intestinal phase, which may be ascribed to the disruption of the micellar casein structure upon the action of the pancreatic enzymes (Huppertz, Vaia, & Smiddy, 2008; Ozel et al., 2020). In the case of the aerogels, the structure was substantially different depending on the polysaccharide. While the agar aerogels showed a fluffier appearance, the κ-carrageenan aerogels were clearly shrunk forming more collapsed and denser structures, especially in the case of aerogels with the greatest polysaccharide ratio. The greater susceptibility of agar aerogels to rehydration was also observed in pure polysaccharide aerogels which were rehydrated in SGF (Figure S1). Interestingly, all the aerogels were highly re-hydrated during the digestions, allowing the diffusion of the gastric and intestinal fluids into the aerogel structure and producing solid fractions with a similar consistency to that from the hydrogels. This is not unexpected, since previous studies have demonstrated the great sorption capacity of polysaccharide-based aerogels (Benito-González, López-Rubio, Gómez-Mascaraque, & Martínez-Sanz, 2020; Fontes-Candia, Erboz, Martínez-Abad, López-Rubio, & Martínez-Sanz, 2019). In fact, sorption experiments showed that the aerogels were able to sorb relatively high amounts of liquid when soaked in SGF (cf. Figure S2), reaching their

maximum sorption values after approximately 60 min, with >30 g SGF/g aerogel for AG-A75, ~25 g SGF/g aerogel for AG-KC25, ~23 g SGF/g aerogel for AG-A25 and ~15 g SGF/g aerogel for AG-KC75. The sorption capacity of the aerogels is expected to be highly relevant, since a limited sorption of the SGF would impede a proper diffusion of the digestive enzymes into the aerogels through the liquid media. While in the case of κ-carrageenan an increase in the polysaccharide content reduced the sorption capacity of the aerogels due to the formation of very compacted and shrunk structures, the opposite was noted in the case of the agar aerogels, with the AG-A75 presenting the greatest SGF sorption capacity of all the samples. In fact, due to its high sorption capacity, when AG-A75 was incubated in the SGF it was capable of retaining the whole volume of liquid within its structure and thus, only a solid phase, corresponding to the re-hydrated aerogel, was obtained after the gastric digestion. This can also be linked to the morphology of the aerogels, which was characterized by SEM and representative images are shown in Figure S3. As observed, in the case of agar an increase in the polysaccharide ratio led to a more open porous structure. However, in the case of κ-carrageenan, the shrinkage of the aerogels observed when increasing the polysaccharide content was also reflected in the microstructure, noting a more heterogeneous porous structure where some of the pores were disrupted. Previous studies have demonstrated that more porous polysaccharide-based aerogels are able to sorb greater amounts of liquid than those presenting a more compacted structure (Benito-González et al., 2020; Fontes-Candia et al., 2019). This may explain the greater capacity of AG-A75 to sorb and retain SGF within its structure.

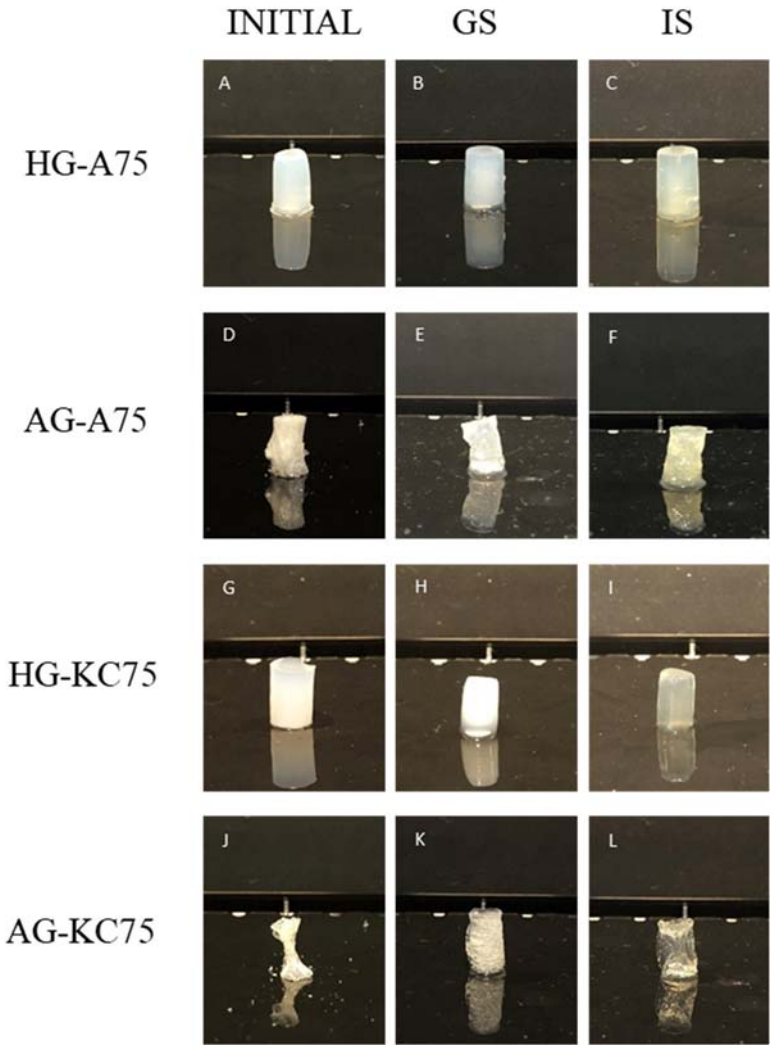

Figure 1. Visual appearance of the initial (A, D, G and J) polysaccharide-casein hydrogels (HG) and aerogels (AG) with a polysaccharide:protein ratio of 75:25, and the corresponding gastric (GS) (B, E, H and K) and intestinal (IS) (C, F, I, and L) solid phases.

The solid and liquid fractions obtained after the gastric and intestinal digestion of all the samples were characterized by means of elemental analysis to determine their protein content and the obtained results, together with the corresponding dry weight fractions, are summarized in Table S1. The estimated dry weight fractions for the

358 liquid and solid phases obtained from the gel-like structures evidence that during the
359 gastric phase all the samples were able to sorb part of the SGF, leading to solid weight
360 fractions higher than the theoretical values expected if no sorption had taken place
361 (60% w/w in the formulations with a polysaccharide:protein ratio of 75:25 and 33%
362 w/w in the formulations with a polysaccharide:protein ratio of 25:75). In contrast,
363 during the intestinal phase the sorption of the SIF seemed to be limited, significantly
364 increasing the weight fraction in the liquid phase. Interestingly, while the solid weight
365 fractions for the gel-like structures with a polysaccharide:protein ratio of 75:25 were
366 generally higher than the theoretical value (i.e., 43% w/w), the opposite trend was
367 observed for the formulations with a polysaccharide:protein ratio of 25:75, with solid
368 weight fractions lower than expected (i.e., 20% w/w). This indicates that the structural
369 integrity of the gel-like structures with lower polysaccharide content was partially lost
370 during the intestinal digestion, which is reasonable since the polysaccharide is the main
371 structuring component in the developed gel-like structures.
372
373 The protein distribution in the solid and liquid phases, after the gastric and intestinal
374 digestions of the gel-like structures, were determined and the results are displayed in
375 Figure 2. According to the results, the hydrogels from both polysaccharides behaved
376 similarly during the gastric phase, with at least half of the total protein content
377 remaining in the solid fraction. The hydrogels with a polysaccharide:protein ratio of
378 75:25 presented greater protein content in the solid fraction than the 25:75 hydrogels
379 which could be ascribed to a greater diffusion of the casein towards the liquid medium
380 in the hydrogels with the lower structuring polysaccharide content. This effect was
381 also observed in the case of the aerogels. On the other hand, in general, the protein

content in the solid fraction from the aerogels after the gastric phase was similar or lower than that from the corresponding hydrogels (except for the AG-A75 in which there was only one solid phase containing all the protein), suggesting that the physical state of the matrix had a strong effect on the release of the casein from the gel-like structures.

After the intestinal phase, the protein content in the liquid fraction increased in all the samples, especially in the gel-like structures with a polysaccharide:protein ratio of 25:75. This, together with the calculated weight fractions, suggests that a greater amount of protein was released during the intestinal phase for these materials as compared to the 75:25 formulations. These results could be ascribed to the fact that a lower concentration of gelling polysaccharides generally leads to the formation of weaker gel structures (Fontes-Candia, Ström, Gómez-Mascaraque, et al., 2020). Indeed, as shown in Table S2, the estimated gel strength values were significantly lower (6-7-fold) when reducing the polysaccharide content from 75% to 25%, regardless of the type of polysaccharide. Thus, the gel-like structures with a polysaccharide:protein ratio of 25:75 are expected to promote a greater release of the casein and be more susceptible to disintegration upon the gastrointestinal digestion conditions. In fact, Koutina et al. reported that at low alginate:protein ratios, there was not sufficient alginate to create a shielding effect able to delay or even prevent the digestion of the protein, while at high alginate:protein ratios whey proteins were protected from pepsin digestion (Koutina, Ray, Lametsch, & Ipsen, 2018).

405

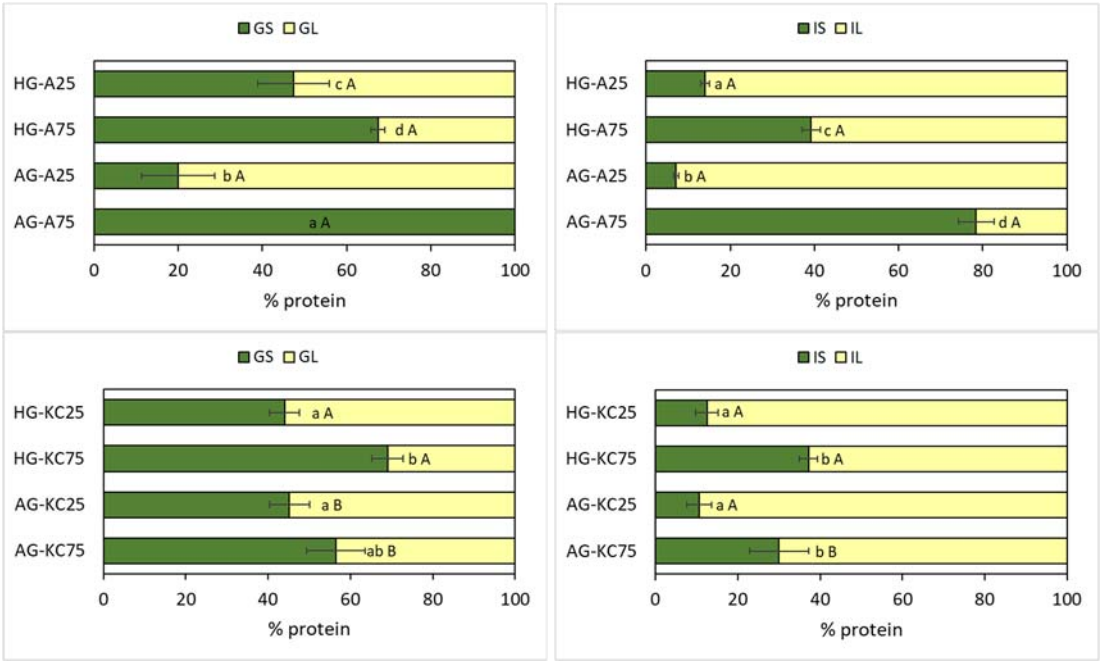

406

407 **Figure 2.** Protein content distribution in the solid (S) and liquid (L) fractions after the
408 gastric (G) and intestinal (I) digestion phases for the agar (A) (top) and κ-carrageenan
409 (KC) (bottom) hydrogel (HG) and aerogel (AG) formulations with a
410 polysaccharide:protein ratio of 25:75 and 75:25 (coded as 25 and 75, respectively).
411 Different lowercase letters (a, b, c, d) indicate statistically meaningful differences
412 ($p \leq 0.05$) between the protein content in the liquid fraction from each graph (i.e.,
413 samples with the same polysaccharide type and at the same digestive stage). Different
414 capital letters (A, B, C, D) indicate statistically meaningful differences ($p \leq 0.05$)
415 between the protein content in the liquid fraction from agar and κ-carrageenan
416 formulations (for samples with the same physical state, polysacharide:protein ratio and
417 digestive stage).

418

419 To investigate the evolution of the microstructure during the gastrointestinal
420 digestions, the polysaccharide-casein gel-like structures, as well as the control
421 samples, and the digested materials obtained after the gastric and intestinal phases

were examined by means of CLSM, using a specific staining agent for the protein, and representative images are shown in Figure 3. As observed, the control casein showed a well-defined structure of spherically-shaped particles (cf. Figure S4) with heterogeneous size distribution (average diameter of ca. 30.3 ± 24.6 μm). Such particles correspond to aggregated casein, i.e. casein clusters, which are known to be formed in commercial caseinate powders as a result of ionic interactions (Jarunglumlert, Nakagawa, & Adachi, 2015). After the gastric digestion, these characteristic structures were almost completely disrupted, with the remaining protein forming heterogeneous aggregates with a relatively large size. After the intestinal phase, the casein seemed to be completely digested and only very small structures (ca. 5.8 ± 1.9 μm) could be visualized, which most likely corresponded to aggregates of the digestive enzymes (cf. Figure S4). Surprisingly, the presence of a small fraction of polysaccharide (i.e., polysaccharide:protein ratio of 25:75) had a significant impact on the microstructure of the digested samples, giving rise to completely different microstructures depending on the added polysaccharide. While in the presence of agar the digested protein was detected as a diffused network of small particles both after the gastric and intestinal digestions, the addition of κ-carrageenan led to the formation of protein aggregates similar to those observed in the control casein after the gastric digestion, but larger protein fragments were detected after the intestinal digestion. This suggests that the establishment of polysaccharide-casein interactions may have an effect on the digestion of the protein and the nature of these interactions is dependent on the type of polysaccharide (Markussen et al., 2021). In particular, it seems that the negative charges provided by the sulphate groups in the agar promoted the formation of polysaccharide-protein complexes at the acidic conditions of the gastric digestion

446 phase, while in the case of the κ-carrageenan, the inclusion of K^+ ions (added to
447 stabilize the gel networks) precluded from this effect and instead, protein and
448 polysaccharide phases separated.
449
450 With respect to the polysaccharide-casein gel-like structures, the microstructure of the
451 digested samples was seen to be different depending on the physical state of the matrix
452 and the gelling polysaccharide. Figure 3A compiles the images corresponding to the
453 agar-based gel-like structures and the solid fractions obtained after the gastric and
454 intestinal digestions. The intact casein clusters could be clearly visualized in the HG-
455 A25 hydrogel; however, in the case of HG-A75 and of the aerogels, the protein did not
456 seem to be properly stained (although in some cases the clusters could be visualized in
457 the images as solid non-stained particles). The reason for this distinct staining of the
458 protein in the samples is unknown and could be due to diffusion effects or to a lower
459 amount of reactive functional groups in some of the samples due to the formation of
460 protein-polysaccharide complexes. After the gastric phase, some intact casein clusters
461 could be detected in the solid fraction from HG-A25 and AG-A75, while smaller
462 protein fragments were visualized in HG-A75. In line with the protein distribution
463 results, CLSM images show that a significant amount of casein remains in the solid
464 fraction. These results are indicative of a protective effect of these structures during
465 the gastric digestion, limiting the disruption of the casein aggregates as it occurred in
466 the non-complexed casein. After the intestinal digestion, casein clusters were not
467 detected, suggesting that the protein remaining in the solid fraction had been
468 extensively digested; however, larger structures were observed in HG-A75 and AG-

A75. This might be due to a lower extent of digestion in the remaining casein or to the establishment of interactions between the digested casein and the agar.

The κ-carrageenan gel-like structures and the solid fractions from their digests were also analysed and representative images are shown in Figure 3B**.** Similarly to the agar-based structures, casein aggregates were clearly visualized in HG-KC25, while the strongly compacted structure of the other samples impeded a proper staining and visualization of the casein. Examination of the solid fractions obtained after the gastric digestions suggested that a greater proportion of protein was released towards the liquid medium in the case of the aerogels, which is in agreement with the protein distribution results (cf. Figure 2). Intact casein clusters were observed in the solid fraction from HG-KC75 and a few smaller fragments were detected in AG-KC25 and AG-KC75. Interestingly, the structure of casein aggregates could be unequivocally seen in the solid fraction from HG-KC25 but the staining agent did not seem to penetrate towards the interior of the clusters and the surface regions appear with a green coloration instead. This might be attributed to strong polysaccharide-protein interactions impeding a proper penetration of the staining agent. After the intestinal phase, few clusters could be still detected in the solid from HG-KC75, indicating that the strong hydrogel network structure formed in this case (Table S2) limited the release of the casein towards the liquid phase. Smaller particles were detected in the solids from HG-KC25, AG-KC25 and AG-KC75, similarly to what was observed in the intestinal solids from the agar-based gel-like structures.

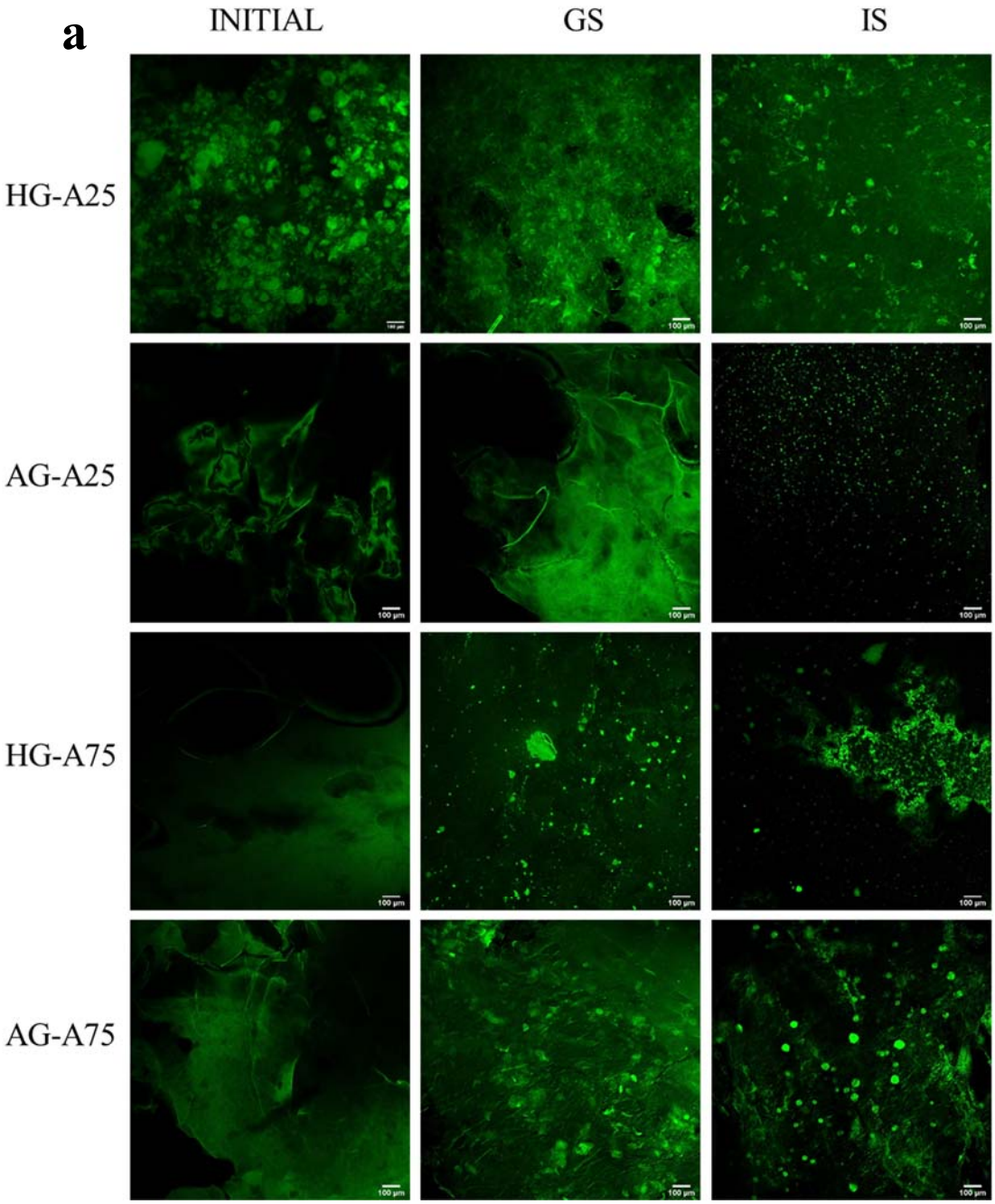

492

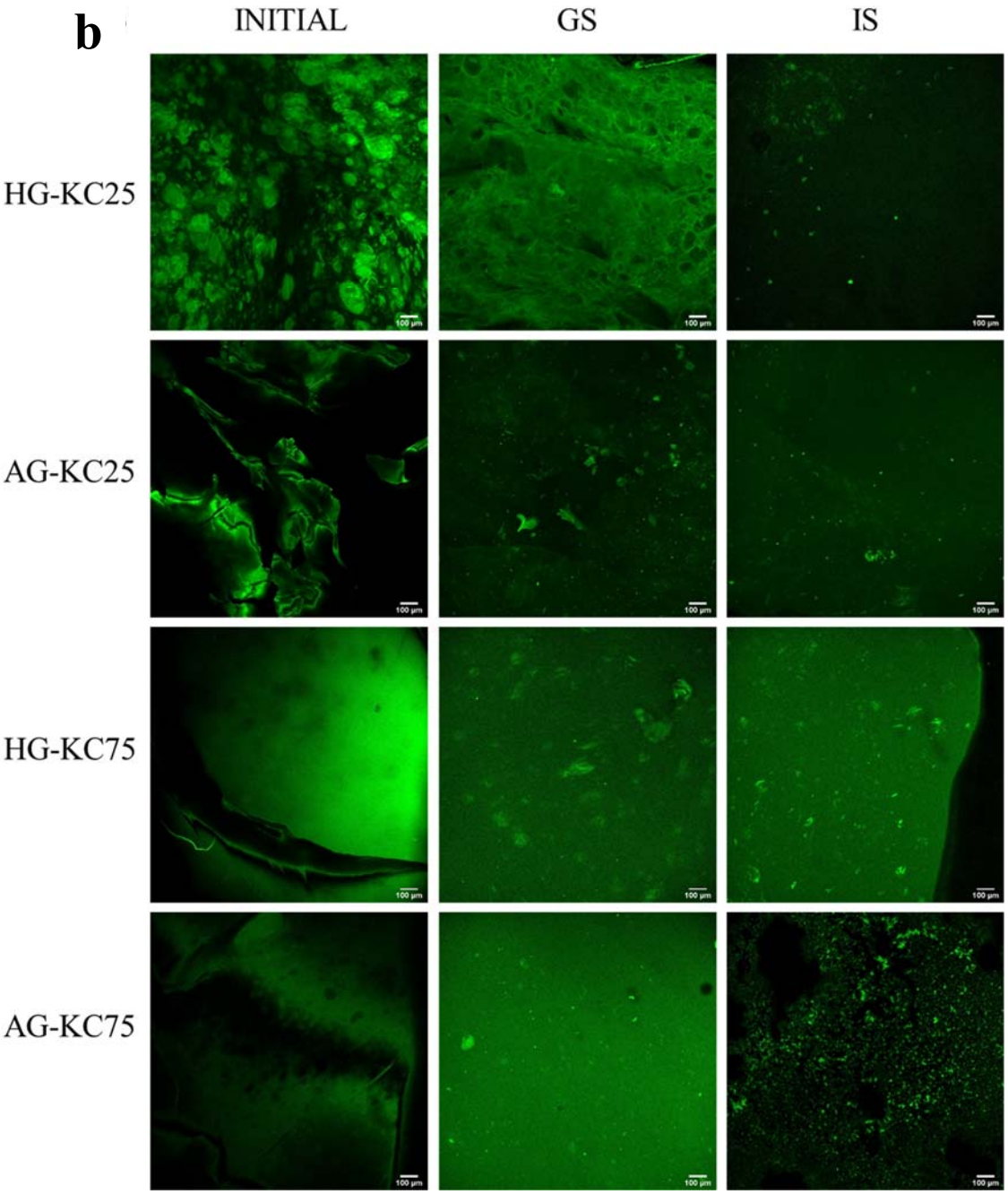

493

494 **Figure 3.** Confocal laser microscopy images of the initial polysaccharide-casein
495 hydrogel (HG) and aerogel (AG) structures and their corresponding solid fractions
496 generated after the gastric (GS) and intestinal (IS) digestion phases. The images shown
497 in (a) correspond to the agar-based (A) formulations and the images in (b) correspond
498 to the κ-carrageenan-based (KC) formulations with a polysaccharide:protein ratio of
499 25:75 and 75:25 (coded as 25 and 75, respectively).

3.2. Protein degradation upon gastrointestinal *in-vitro* digestion

Casein degradation during simulated gastrointestinal digestion was followed by studying the molecular weight (MW) distribution of proteins and peptides above 10 kDa through SDS-PAGE. Figures 4A and 4B show the obtained protein profiles after the gastric and intestinal digestions. The bands corresponding to the control casein were observed between 25 and 37 kDa, which correspond to the α_{s1}-casein, α_{s2}-casein, β-casein and κ-casein (Egger et al., 2016). A band was also observed around 18 kDa, which corresponds to the residual serum protein β-lactoglobulin (Li et al., 2020) As expected, after the gastric digestion the casein characteristic bands were absent in the non-complexed protein and instead the presence of β-lactoglobulin and peptides with MW < 10 kDa was noted. After the subsequent intestinal digestion only the bands corresponding to the added pancreatic enzymes (porcine pancreatic lipase (50 kDa), trypsin (23.3 kDa), chymotrypsin (25.5-29.10 kDa) and elastase (25.9 kDa) could be detected (Sanchón et al., 2018), suggesting that the protein had been digested into small peptide fragments. The casein degradation observed after the gastric phase is in agreement with other works (Egger et al., 2016; Sanchón et al., 2018) and it is explained by the flexible and open structure of casein, leading to a higher sensitivity to proteolysis (Li et al., 2020).

After the gastric digestion, the casein characteristic bands were clearly observed in the solid fractions from the hydrogels (HG-A25 and HG-A75) and less evidently in the aerogel AG-A75. In agreement with CLSM, this confirms the presence of non-digested casein which is retained within the structure of these materials. It should be noted that in the case of AG-A75 the bands were less clearly discerned and the whole well was

524 stained. This can be attributed to interference of the polysaccharide due to casein-
525 polysaccharide interactions being established. Sample handling was indeed more
526 complex due to the higher viscosity of this material. After the intestinal phase, the
527 casein bands were absent in all the samples; however, peptides with MW < 10 kDa
528 were observed in most of them, appearing this region more intensely stained in C-A75,
529 the liquid from HG-A25, HG-A75 and AG-A75, as well as the solid phase from AG-
530 A75. This suggests a lower degree of casein hydrolysis during the intestinal digestion
531 in these samples.
532
533 The SDS-PAGE profile of the digests from the κ-carrageenan gel-like structures are
534 shown in Figure 4B. As observed, after the gastric digestion the characteristic bands
535 of intact casein were present in the solid fraction from the hydrogels (HG-KC25 and
536 HG-KC75), as well as the liquid from HG-KC75. Once again, handling some of these
537 samples was extremely complex due to their high viscosity and, in some cases such as
538 for the AG-KC25 sample, polysaccharide interference impeded a proper visualization
539 of the electrophoretic bands. After the intestinal digestion, all the samples showed a
540 very similar profile to that from the non-complexed casein, suggesting that the κ-
541 carrageenan structures did not exert a significant protective effect against the effect of
542 the pancreatin. It should be noted that although intact casein clusters were detected in
543 the CLSM images from the intestinal solid from HG-KC75, no signs of protein were
544 seen in the corresponding well. This may be explained by the remaining clusters being
545 strongly interacting with the polysaccharide network, hence being separated upon
546 sample preparation and not able to migrate into the electrophoresis gel. Thus, it should
547 be taken into consideration that the SDS-PAGE results are not conclusive since (i)

548 higher polysaccharide contents in some of the samples could hinder the migration of
549 the protein through the gel and (ii) polysaccharide-protein complexes may have not
550 been properly detected due to polysaccharide interference. A possible strategy to avoid
551 this and improve the accuracy of the SDS-PAGE results would be the use of specific
552 enzymes to hydrolyse and separate the polysaccharides, hence allowing a proper
553 identification of the whole protein fraction remaining in the samples.
554
555 These results, together with CLSM, suggest that some of the developed gel-like
556 structures exerted a strong protective effect during the gastric digestion, being able to
557 retain a fraction of non-digested casein clusters in the solid phase. In general, the
558 hydrogels limited to a greater extent the release of casein towards the liquid medium
559 and showed a greater protective effect than the aerogels. Despite the high sorption
560 capacity of AG-A75, this specific structure also resulted in a notable protective
561 capacity. Moreover, the polysaccharide:protein ratio seems to be highly relevant, with
562 higher ratios limiting the digestion of casein even during the intestinal phase.
563

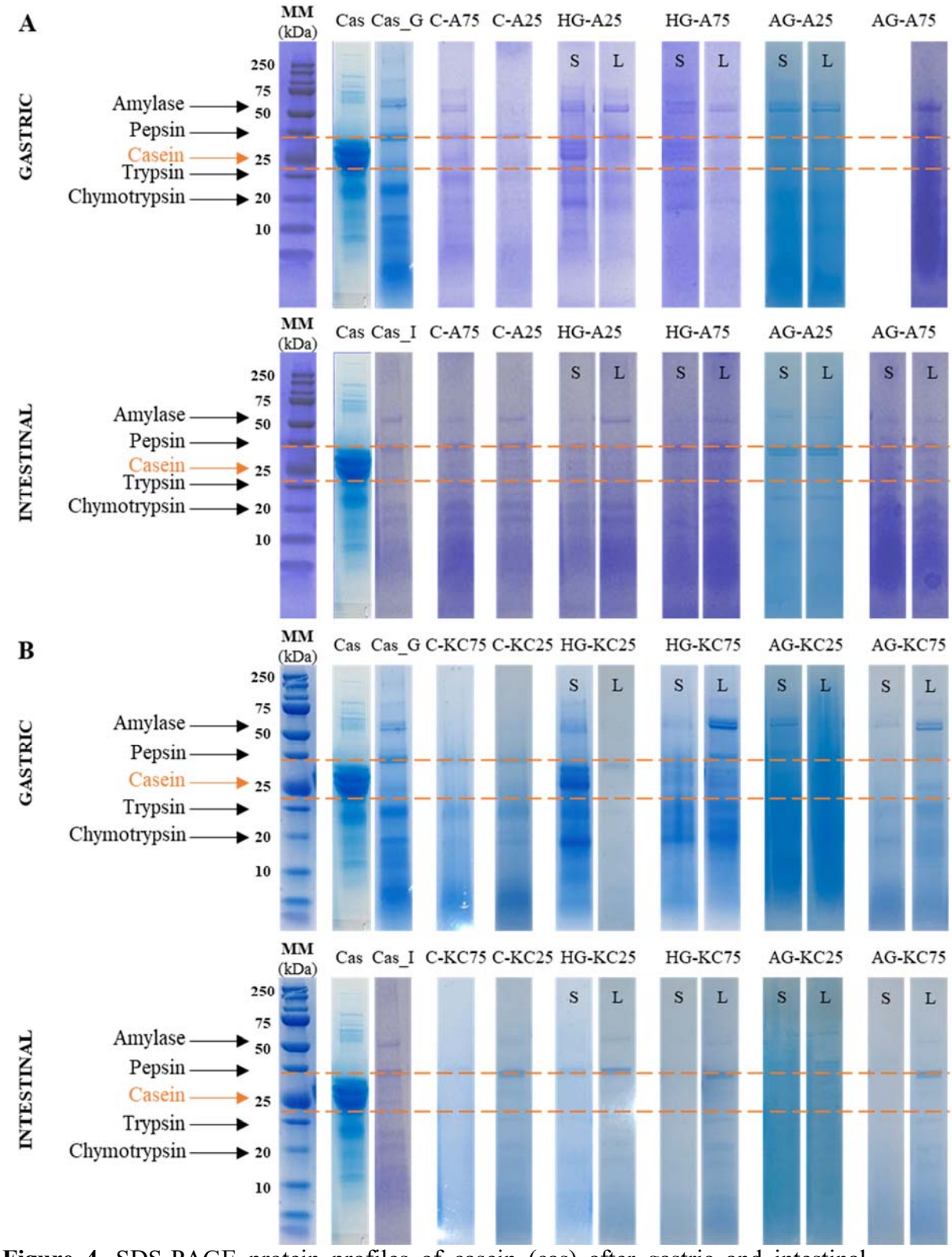

564

565

566 **Figure 4.** SDS-PAGE protein profiles of casein (cas) after gastric and intestinal

567 digestion of agar (A) and κ-carrageenan (KC) (A and B, respectively) hydrogels (HG)

568 and aerogels (AG) with a polysaccharide:protein ratio of 25:75 and 75:25 (coded as 25
569 and 75, respectively). MW: molecular weight marker; S: solid phase; L: liquid phase.
570
571 In order to evaluate the MW distribution of the intestinal digestion-derived peptides
572 from the polysaccharide-casein gel-like structures, the samples were characterized by
573 MALDI-TOF and the results, expressed as the percentage of peptides within a given
574 MW range, are shown in Figure 5. As observed, in most of the samples the majority
575 of the peptides detected were within the low MW range (0.5-1 kDa), while less than
576 30% of the peptides showed MW>4 KDa. Interestingly, the MW distribution of the
577 peptides detected in the gastrointestinal digests from the polysaccharide-casein gel-
578 like structures varied depending on the type of polysaccharide. In particular, digests
579 from κ-carrageenan presented a greater percentage of peptides within the range of 0.5-
580 1 kDa than those from the non-complexed casein and from the agar samples. On the
581 other hand, species larger than 18 kDa, that is whole proteins, were found in the κ-
582 carrageenan digests, while proteins within this MW range could not be detected in the
583 agar samples, except in AG-A25. This might be indicative of the presence of a small
584 fraction of casein being strongly bound to κ-carrageenan, hence being less susceptible
585 to the hydrolytic effect of pepsin and pancreatic enzymes. For both polysaccharides,
586 the MW distribution of the peptides was dependent on the polysaccharide:protein ratio
587 and the physical state of the gel-like structures. Thus, while a greater percentage of
588 peptides with MW>2 kDa was observed in the aerogels with higher polysaccharide
589 content (75:25 ratio), the opposite effect was noted in the hydrogels. Overall, the agar-
590 based gel-like structures seemed to provide a greater release of peptides within the
591 range of MW>2 kDa towards the liquid media.

Linking these results with CLSM, it seems that the strong network originated in the hydrogels with the higher polysaccharide:protein ratio (75:25), especially in the case of κ-carrageenan, provided a great protection against the digestion of casein, with larger protein fragments remaining in the solid fraction even after the intestinal phase. In that case, reducing the polysaccharide:protein ratio to 25:75 seemed to be beneficial to promote the release of casein during the intestinal phase towards the liquid medium and provide a greater relative amount of peptides with MW>2 kDa. On the other hand, the porous structure of the aerogels seemed to provide a greater release of the casein towards the liquid medium, limiting the protective effect of these type of structures. Thus, increasing the polysaccharide:protein ratio to 75:25 would be positive in that case to generate stronger and more compact structures. The stronger networks originated in the case of κ-carrageenan are due to the gelation mechanism induced by the presence of added cations (K^+) which lead to the formation of strong ionic interactions, as opposed to the agar networks, which are solely held by means of hydrogen bonding (Fontes-Candia et al., 2021). Upon freeze-drying, the κ-carrageenan networks are strongly collapsed, forming very compact aerogels which would be less suitable for a sustained release of the casein than the more porous structure of the agar-based aerogels (cf. Figure S2).

612

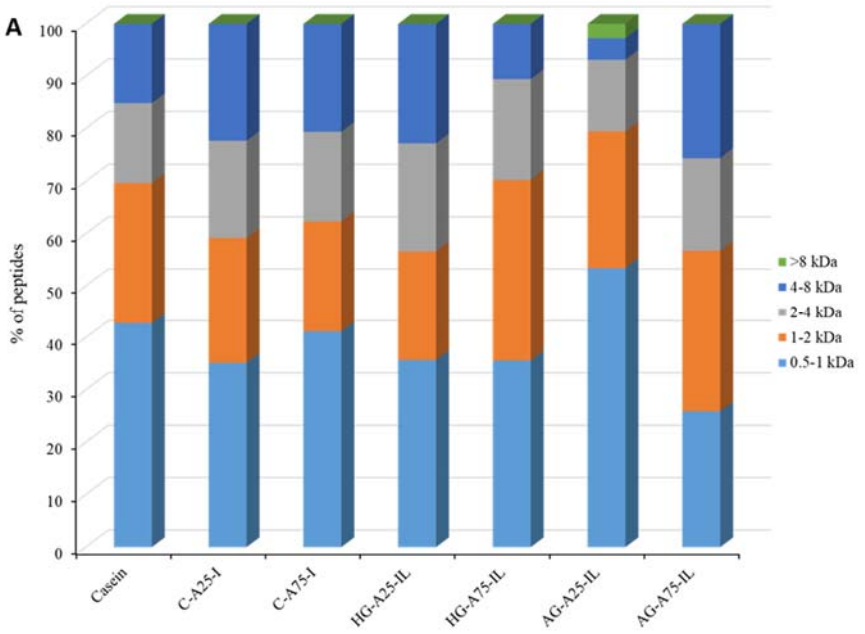

613

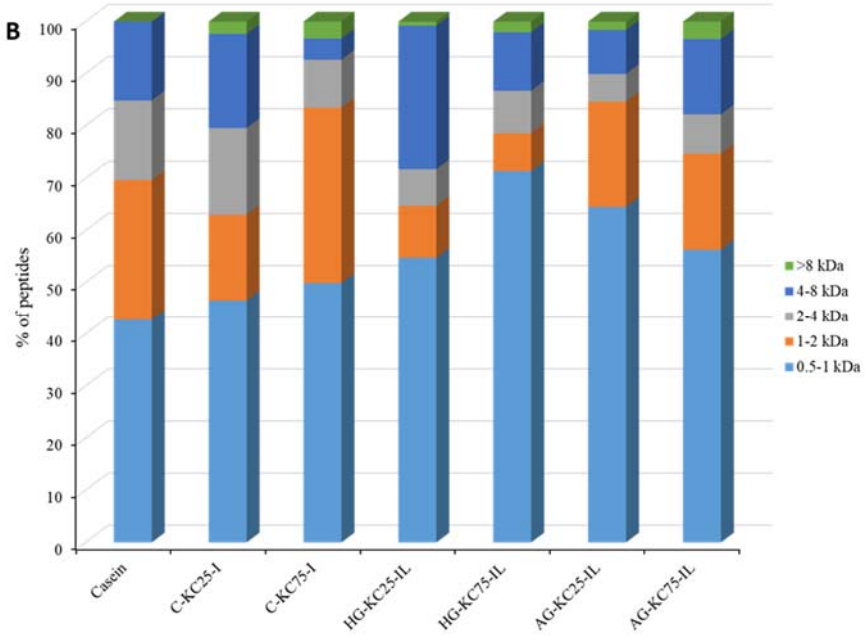

614 **Figure 5**. Molecular weight distribution expressed as the relative fraction of casein
615 peptides detected in the intestinal phase (I) of the control samples and the liquid
616 intestinal fractions (IL) from the agar (A) and κ-carrageenan (KC) (A and B,
617 respectively) hydrogel (HG) and aerogel (AG) structures with a polysaccharide:protein
618 ratio of 25:75 and 75:25 (coded as 25 and 75, respectively) in comparison to casein.

3.3. Peptidomic characterization of intestinal *in-vitro* digests

Digested casein and the liquid fractions from the gel-like structures with the highest protein content were analysed by HPLC-MS/MS after the gastrointestinal digestion. All the peptides identified for each sample were simultaneously compared and the results are represented in a Venn diagram (cf. Figure 6). As observed, the amount of peptides detected in the polysaccharide:casein hydrogels at the end of the intestinal digestion was greater than in the control casein, which may be due to a certain degree of protection of the hydrogel structures against the hydrolytic enzymes. Furthermore, the peptide sequences detected in the digests from the hydrogels were significantly different to those observed in the control casein, since only a small overlapping region of the total number of peptides was noted. The longer peptide sequences detected in the hydrogel samples suggest that the microstructure of these materials seems to be optimum to delay casein digestion during the gastric phase, while allowing the release and hydrolysis of casein during the intestinal phase. Contrarily, for the aerogel structures the amount of detected peptides was lower than the control casein. This could be related to the greater release of protein which took place in these samples during the gastric phase, leading to a greater casein hydrolysis. When evaluating the obtained results, the limitations of the HPLC-MS/MS analyses should be taken into consideration. Firstly, all those compounds which are not completely soluble in the solvent (water:formic acid) are removed during sample preparation; this means that the protein bound to polysaccharides is discarded. In this regard, the use of specific enzymes to hydrolyse the polysaccharide fraction, prior to the analyses, could be useful. Additionally, the instrumental conditions favour the detection of peptides with MW between 0.5 and 3 kDa, although a few peptides with longer sizes could be

643 identified depending on their ionization capacity. Thus, long peptide fragments are not
644 expected to be detected by HPLC-MS/MS since they may not be properly solubilized
645 or ionized.
646
647 Most of the identified peptides corresponded to sequences from β-casein and α_{s1}-
648 casein, with minor amounts of peptides corresponding to α_{s2}-casein. The peptide
649 patterns, color-coded to represent the abundance of amino acids identified along the
650 protein sequence for the β-, and α_{s1}-casein are represented in Figure S5. The patterns
651 for the control casein at the end of the intestinal digestion are similar to previously
652 reported data (Ana-Isabel Mulet-Cabero et al., 2020; Bohn et al., 2017; Egger et al.,
653 2019) and confirm that this protein fraction undergoes a high degree of degradation
654 during digestion. A greater amount of peptides within the region ^{62}FPGPI^{66} and
655 ^{150}PLPPT^{154} from β-casein were observed for all the samples, while the region
656 ^{73}NIPPL^{77} also presented higher abundance of peptides for the control casein and HG-
657 A25. Interestingly, a greater amount of peptides were detected within different regions
658 in the intestinal liquid from each particular gel-like structure. For instance, in the case
659 of HG-KC25 the ^{120}TESQSLTLTDVEN^{132} and ^{160}QSVLS^{164} regions appeared more
660 intense than in the control casein, while the ^{33}FQSEEQQQTEDELQDKIHP^{51} region
661 was more intense in AG-A25. In the case of the α_{s1}-casein, the ^{65}ISSS^{68} and the C-
662 terminal region ^{182}IPNPI^{187} were consistently detected in all the samples. Notably,
663 peptide fragments from the region ^{65}ISSSEEIVPNSVEQKHIQKEDV^{86} were highly
664 abundant in the intestinal liquid from AG-A25, while peptides within the region
665 ^{50}EDQAMEDIKQMEAESIS^{66} were more abundant in HG-KC25. Overall, the results
666 confirm the protective effect of both hydrogels, limiting the hydrolysis of casein and

promoting the release of longer soluble peptide sequences. This was especially noted in the case of HG-KC25, which may be explained by the greater proportion of peptides with lower MW in this sample, as evidenced by the MALDI-TOF results. The peptides with higher MW present in the intestinal liquid from HG-KC25 may have not been detected by HPLC-MS/MS due to the already mentioned limitations of this technique. It should be noted that in the particular case of AG-A25, despite the greater release of casein during the gastric phase, leading to greater casein hydrolysis, a small proportion of casein may have still remained tightly bound to the polysaccharide, being hydrolysed during the intestinal phase and giving rise to longer peptides within specific regions of the protein sequence.

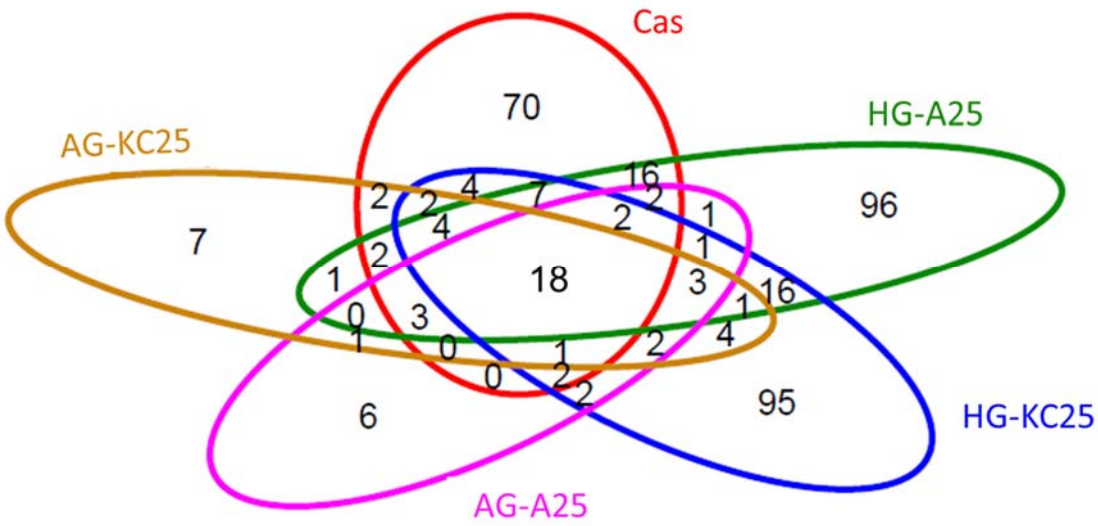

Figure 6. Venn diagrams of the peptide sequences identified in the intestinal digests from selected polysaccharide-protein hydrogel (HG) and aerogel (AG) structures and the control casein (Cas) with a polysaccharide:protein ratio of 25:75.

4. Conclusions

Polysaccharide-casein gel-like structures (hydrogels and aerogels) were able to affect the hydrolysis of casein upon *in-vitro* gastrointestinal digestions, being this effect dependent on the polysaccharide type, the polysaccharide:casein ratio and the physical state of the structures. Although the mere presence of the sulphated polysaccharides seemed to produce a slight protective effect against the hydrolysis of casein during the gastric phase, this effect was maximized by the development of gel-like structures.

During the gastric phase all the developed structures kept their physical integrity and the aerogels were able to sorb SGF to rehydrate. Non-digested casein, in the form of clusters, was seen to remain in the solid fraction from most of the samples after the gastric phase, while smaller particles were observed in the solids obtained at the end of the intestinal digestion. In general, the hydrogels limited to a greater extent the release of casein towards the liquid medium and showed a greater protective effect than the aerogels, except for AG-A75. Moreover, lower polysaccharide concentration yielded softer gels with less physical integrity and more prone to release the protein.

HG-A25, AG-A75 and HG-KC25 were determined as the most optimal structures for the intended application, since they were able to preserve intact casein after the gastric phase while promoting the release of peptides with greater molecular weights during the intestinal phase. These results evidence the potential of polysaccharide-protein gel-like structures to produce satiating dietary products and demonstrate the relevance of their structural properties on their behavior upon digestion.

Acknowledgements

The projects RTI2018-094268-B-C22 and RTI2018-094408-J-I00 were funded by MCIN/AEI/10.13039/501100011033 and by "ERDF A way of making Europe". This work has also received financial support from project PID2019-107663RB-I00 from the Spanish Ministry of Science and Innovation (MICINN). Cynthia Fontes-Candia is recipient of a pre-doctoral grant from CONACYT (MEX/Ref. 306680).

References

Agostinho, D. A. S., Paninho, A. I., Cordeiro, T., Nunes, A. V. M., Fonseca, I. M., Pereira, C., … Ventura, M. G. (2020). Properties of κ-carrageenan aerogels prepared by using different dissolution media and its application as drug delivery systems. *Materials Chemistry and Physics*, *253*, 123290. https://doi.org/10.1016/J.MATCHEMPHYS.2020.123290

Alavi, F., Emam-Djomeh, Z., Yarmand, M. S., Salami, M., Momen, S., & Moosavi-Movahedi, A. A. (2018). Cold gelation of curcumin loaded whey protein aggregates mixed with k-carrageenan: Impact of gel microstructure on the gastrointestinal fate of curcumin. *Food Hydrocolloids*, *85*, 267–280. https://doi.org/10.1016/j.foodhyd.2018.07.012

Ana-Isabel Mulet-Cabero, Lotti Egger, Reto Portmann, Olivia Ménard, Sébastien Marze, Mans Minekus, … Alan Mackie. (2020). A standardised semi-dynamic in vitro digestion method suitable for food – an international consensus. *Food & Function*, *11*(2), 1702–1720. https://doi.org/10.1039/C9FO01293A

Apong, P. E. (2019). Nutrition and Dietary Recommendations for Bodybuilders. *Nutrition and Enhanced Sports Performance*, 737–750.

731 Benito-González, I., López-Rubio, A., Gómez-Mascaraque, L. G., & Martínez-Sanz,
732 M. (2020). PLA coating improves the performance of renewable adsorbent pads
733 based on cellulosic aerogels from aquatic waste biomass. *Chemical Engineering*
734 *Journal*, 124607.
735 Bohn, T., Carriere, F., Day, L., Deglaire, A., Egger, L., Freitas, D., … Dupont, D.
736 (2017). Correlation between in vitro and in vivo data on food digestion. What can
737 we predict with static in vitro digestion models?
738 *Https://Doi.Org/10.1080/10408398.2017.1315362*, *58*(13), 2239–2261.
739 https://doi.org/10.1080/10408398.2017.1315362
740 Brodkorb, A., Egger, L., Alminger, M., Alvito, P., Assunção, R., Ballance, S., …
741 Recio, I. (2019). INFOGEST static in vitro simulation of gastrointestinal food
742 digestion. *Nature Protocols*, *14*(4), 991–1014. https://doi.org/10.1038/s41596-
743 018-0119-1
744 Caron, J., Cudennec, B., Domenger, D., Belguesmia, Y., Flahaut, C., Kouach, M., …
745 Ravallec, R. (2016). Simulated GI digestion of dietary protein: Release of new
746 bioactive peptides involved in gut hormone secretion. *Food Research*
747 *International*, *89*, 382–390. https://doi.org/10.1016/J.FOODRES.2016.08.033
748 Dallas, D. C., Sanctuary, M. R., Qu, Y., Khajavi, S. H., Van Zandt, A. E., Dyandra,
749 M., … German, J. B. (2017). Personalizing protein nourishment. *Critical Reviews*
750 *in Food Science and Nutrition*, *57*(15), 3313–3331.
751 de Jong, S., Klok, H. J., & van de Velde, F. (2009). The mechanism behind
752 microstructure formation in mixed whey protein–polysaccharide cold-set gels.
753 *Food Hydrocolloids*, *23*(3), 755–764.
754 https://doi.org/10.1016/J.FOODHYD.2008.03.017

Egger, L., Ménard, O., Baumann, C., Duerr, D., Schlegel, P., Stoll, P., … Portmann, R. (2019). Digestion of milk proteins: Comparing static and dynamic in vitro digestion systems with in vivo data. *Food Research International*, *118*, 32–39. https://doi.org/10.1016/J.FOODRES.2017.12.049

Egger, L., Ménard, O., Delgado-Andrade, C., Alvito, P., Assunção, R., Balance, S., … Portmann, R. (2016). The harmonized INFOGEST in vitro digestion method: From knowledge to action. *Food Research International*, *88*, 217–225. https://doi.org/10.1016/j.foodres.2015.12.006

Fontes-Candia, C., Erboz, E., Martínez-Abad, A., López-Rubio, A., & Martínez-Sanz, M. (2019). Superabsorbent food packaging bioactive cellulose-based aerogels from Arundo donax waste biomass. *Food Hydrocolloids*, *96*, 151–160.

Fontes-Candia, C., Lopez-Sanchez, P., Ström, A., Martínez, J. C., Salvador, A., Sanz, T., … Martínez-Sanz, M. (2021). Maximizing the oil content in polysaccharide-based emulsion gels for the development of tissue mimicking phantoms. *Carbohydrate Polymers*, *256*, 117496. https://doi.org/https://doi.org/10.1016/j.carbpol.2020.117496

Fontes-Candia, C., Ström, A., Gómez-Mascaraque, L. G., López-Rubio, A., & Martínez-Sanz, M. (2020). Understanding nanostructural differences in hydrogels from commercial carrageenans: Combined small angle X-ray scattering and rheological studies. *Algal Research*, *47*, 101882. https://doi.org/https://doi.org/10.1016/j.algal.2020.101882

Fontes-Candia, C., Ström, A., Lopez-Sanchez, P., López-Rubio, A., & Martínez-Sanz, M. (2020). Rheological and structural characterization of carrageenan emulsion gels. *Algal Research*, *47*, 101873.

https://doi.org/https://doi.org/10.1016/j.algal.2020.101873

Gombotz, W. R., & Wee, S. F. (2012). Protein release from alginate matrices. *Advanced Drug Delivery Reviews*, *64*(SUPPL.), 194–205. https://doi.org/10.1016/J.ADDR.2012.09.007

Huppertz, T., Vaia, B., & Smiddy, M. A. (2008). Reformation of casein particles from alkaline-disrupted casein micelles. *Journal of Dairy Research*, *75*(1), 44–47. https://doi.org/10.1017/S0022029907002956

Jarunglumlert, T., Nakagawa, K., & Adachi, S. (2015). Influence of aggregate structure of casein on the encapsulation efficiency of β-carotene entrapped via hydrophobic interaction. *Food Structure*, *5*, 42–50. https://doi.org/10.1016/J.FOOSTR.2015.05.001

Juvonen, K. R., Karhunen, L. J., Vuori, E., Lille, M. E., Karhu, T., Jurado-Acosta, A., … Herzig, K.-H. (2011). Structure modification of a milk protein-based model food affects postprandial intestinal peptide release and fullness in healthy young men. *British Journal of Nutrition*, *106*(12), 1890–1898. https://doi.org/DOI: 10.1017/S0007114511002522

Koutina, G., Ray, C. A., Lametsch, R., & Ipsen, R. (2018). The effect of protein-to-alginate ratio on in vitro gastric digestion of nanoparticulated whey protein. *International Dairy Journal*, *77*, 10–18. https://doi.org/10.1016/J.IDAIRYJ.2017.09.001

Li, S., Hu, Q., Chen, C., Liu, J., He, G., Li, L., … Ren, D. (2020). Formation of bioactive peptides during simulated gastrointestinal digestion is affected by αs1-casein polymorphism in buffalo milk. *Food Chemistry*, *313*, 126159.

Li, Xianghong, Hua, Y., Qiu, A., Yang, C., & Cui, S. (2008). Phase behavior and

803 microstructure of preheated soy proteins and κ-carrageenan mixtures. *Food*
804 *Hydrocolloids*, *22*(5), 845–853.
805 https://doi.org/10.1016/J.FOODHYD.2007.04.008
806 Li, Xiaoqiang, Su, Y., Liu, S., Tan, L., Mo, X., & Ramakrishna, S. (2010).
807 Encapsulation of proteins in poly(l-lactide-co-caprolactone) fibers by emulsion
808 electrospinning. *Colloids and Surfaces B: Biointerfaces*, *75*(2), 418–424.
809 https://doi.org/10.1016/j.colsurfb.2009.09.014
810 Manzocco, L., Valoppi, F., Calligaris, S., Andreatta, F., Spilimbergo, S., & Nicoli, M.
811 C. (2017). Exploitation of κ-carrageenan aerogels as template for edible oleogel
812 preparation. *Food Hydrocolloids*, *71*, 68–75.
813 https://doi.org/https://doi.org/10.1016/j.foodhyd.2017.04.021
814 Marciani, L., Lopez-Sanchez, P., Pettersson, S., Hoad, C., Abrehart, N., Ahnoff, M.,
815 & Ström, A. (2019). Alginate and HM-pectin in sports-drink give rise to intra-
816 gastric gelation in vivo, *10*, 7892. https://doi.org/10.1039/c9fo01617a
817 Markussen, J. Ø., Madsen, F., Young, J. F., & Corredig, M. (2021). A semi dynamic
818 in vitro digestion study of milk protein concentrate dispersions structured with
819 different polysaccharides. *Current Research in Food Science*, *4*, 250–261.
820 https://doi.org/10.1016/J.CRFS.2021.03.012
821 Martínez-Sanz, M., Ström, A., Lopez-Sanchez, P., Knutsen, S. H., Ballance, S., Zobel,
822 H. K., … López-Rubio, A. (2020). Advanced structural characterisation of agar-
823 based hydrogels: Rheological and small angle scattering studies. *Carbohydrate*
824 *Polymers*, *236*, 115655.
825 https://doi.org/https://doi.org/10.1016/j.carbpol.2019.115655
826 McClements, D. J. (2017). Recent progress in hydrogel delivery systems for improving

827 nutraceutical bioavailability. *Food Hydrocolloids*, *68*, 238–245.
828 https://doi.org/10.1016/J.FOODHYD.2016.05.037
829 Miralles, B., Sanchón, J., Sánchez-Rivera, L., Martínez-Maqueda, D., Le Gouar, Y.,
830 Dupont, D., … Recio, I. (2021). Digestion of micellar casein in duodenum
831 cannulated pigs. Correlation between in vitro simulated gastric digestion and in
832 vivo data. *Food Chemistry*, *343*, 128424.
833 https://doi.org/10.1016/j.foodchem.2020.128424
834 Mouécoucou, J., Villaume, C., Sanchez, C., & Méjean, L. (2004). β-
835 Lactoglobulin/polysaccharide interactions during in vitro gastric and pancreatic
836 hydrolysis assessed in dialysis bags of different molecular weight cut-offs.
837 *Biochimica et Biophysica Acta (BBA) - General Subjects*, *1670*(2), 105–112.
838 https://doi.org/10.1016/J.BBAGEN.2003.10.017
839 Ozel, B., Zhang, Z., He, L., & McClements, D. J. (2020). Digestion of animal- and
840 plant-based proteins encapsulated in κ-carrageenan/protein beads under
841 simulated gastrointestinal conditions. *Food Research International*, *137*, 109662.
842 https://doi.org/https://doi.org/10.1016/j.foodres.2020.109662
843 Putney, S. D. (1998). Encapsulation of proteins for improved delivery. *Current*
844 *Opinion in Chemical Biology*, *2*(4), 548–552. https://doi.org/10.1016/S1367-
845 5931(98)80133-6
846 Sanchón, J., Fernández-Tomé, S., Miralles, B., Hernández-Ledesma, B., Tomé, D.,
847 Gaudichon, C., & Recio, I. (2018). Protein degradation and peptide release from
848 milk proteins in human jejunum. Comparison with in vitro gastrointestinal
849 simulation. *Food Chemistry*, *239*, 486–494.
850 https://doi.org/10.1016/j.foodchem.2017.06.134

Santos-Hernández, M., Tomé, D., Gaudichon, C., & Recio, I. (2018). Stimulation of CCK and GLP-1 secretion and expression in STC-1 cells by human jejunal contents and in vitro gastrointestinal digests from casein and whey proteins. *Food and Function*, *9*(9), 4702–4713. https://doi.org/10.1039/c8fo01059e

Xie, J., & Wang, C.-H. (2007). Encapsulation of proteins in biodegradable polymeric microparticles using electrospray in the Taylor cone-jet mode. *Biotechnology and Bioengineering*, *97*(5), 1278–1290. https://doi.org/10.1002/BIT.21334

Yuan, D., Jacquier, J. C., & O'Riordan, E. D. (2018). Entrapment of proteins and peptides in chitosan-polyphosphoric acid hydrogel beads: A new approach to achieve both high entrapment efficiency and controlled in vitro release. *Food Chemistry*, *239*, 1200–1209. https://doi.org/10.1016/J.FOODCHEM.2017.07.021

Zhang, Z., Zhang, R., & McClements, D. J. (2017). Control of protein digestion under simulated gastrointestinal conditions using biopolymer microgels. *Food Research International*, *100*, 86–94. https://doi.org/10.1016/J.FOODRES.2017.08.037

Zhang, Z., Zhang, R., Zou, L., & McClements, D. J. (2016). Protein encapsulation in alginate hydrogel beads: Effect of pH on microgel stability, protein retention and protein release. *Food Hydrocolloids*, *58*, 308–315. https://doi.org/10.1016/J.FOODHYD.2016.03.015

Supplementary Material

Table S1. Weight fraction, protein content determined by elemental analysis and calculated protein fraction for the solid and liquid fractions from the casein, the

875 polysaccharide-casein controls and the different polysaccharide-casein hydrogels
876 (HG) and aerogels (AG) structures after the gastric (G) and intestinal (I) digestion
877 phases with a polysaccharide:protein ratio of 25:75 and 75:25 (coded as 25 and 75,
878 respectively).

Sample	Phase	Weight fraction (w/w %)	Protein (w/w %)	Protein fraction (w/w %)
Casein	G	100	53.19 ± 0.78	100
	I	100	52.61 ± 0.32	100
C-A25	G	100	53.91 ± 3.83	100
	I	100	52.22 ± 5.80	100
C-A75	G	100	28.00 ± 2.86	100
	I	100	42.39 ± 6.34	100
HG-A25	GS	53.41 ± 8.70	41.80 ± 3.02	47.38 ± 8.50
	GL	46.59 ± 8.70	53.44 ± 3.01	52.62 ± 8.50
	IS	17.26 ± 1.80	42.44 ± 3.72	13.95 ± 1.02
	IL	82.74 ± 1.80	54.42 ± 2.84	86.05 ± 1.02
HG-A75	GS	84.30 ± 0.21	17.62 ± 0.83	67.44 ± 1.57
	GL	15.70 ± 0.21	46.53 ± 2.05	32.56 ± 1.57
	IS	52.96 ± 0.44	28.38 ± 1.802	39.19 ± 2.16
	IL	47.04 ± 0.44	50.76 ± 4.27	60.81 ± 2.16
AG-A25	GS	32.70 ± 5.06	29.93 ± 6.56	20.00 ± 8.62
	GL	67.30 ± 5.06	59.67 ± 1.98	80.00 ± 8.62
	IS	10.73 ± 0.69	30.14 ± 1.52	7.15 ± 0.62

	IL	89.27 ± 0.69	47.12 ± 1.94	92.85 ± 0.62
AG-A75	G	100	21.29 ± 2.32	100
	IS	83.99 ± 0.01	39.31 ± 1.54	78.38 ± 4.26
	IL	16.01 ± 0.01	48.54 ± 2.67	21.62 ± 4.26
C- KC25	G	100	46.69 ± 1.42	100
	I	100	41.52 ± 1.22	100
C- KC75	G	100	24.79 ± 1.02	100
	I	100	39.52 ± 3.37	100
HG-KC25	GS	40.46 ± 6.19	48.67 ± 3.96	44.02 ± 3.66
	GL	59.54 ± 6.19	42.29 ± 6.50	55.98 ± 3.66
	IS	14.33 ± 2.16	37.11 ± 0.78	12.50 ± 2.73
	IL	85.67 ± 2.16	43.52 ± 1.19	87.50 ± 2.73
HG-KC75	GS	83.74 ± 1.29	14.61 ± 1.72	69.01 ± 3.85
	GL	16.26 ± 1.29	33.51 ± 1.72	30.99 ± 3.85
	IS	51.13 ± 1.43	24.68 ± 1.48	37.19 ± 2.20
	IL	48.87 ± 1.43	43.59 ± 1.52	62.81 ± 2.20
AG-KC25	GS	51.46 ± 4.50	44.07 ± 1.16	45.19 ± 4.91
	GL	60.23 ± 4.50	56.60 ± 1.65	54.81 ± 4.91
	IS	13.11 ± 2.93	36.58 ± 2.53	10.61 ± 3.02
	IL	86.89 ± 2.93	46.89 ± 1.51	89.39 ± 3.02
AG-KC75	GS	74.90 ± 5.90	17.41 ± 1.89	56.50 ± 7.12
	GL	25.10 ± 5.90	40.57 ± 4.99	43.50 ± 7.12
	IS	42.41 ± 5.25	25.89 ± 3.81	30.02 ± 7.11
	IL	57.59 ± 5.25	44.54 ± 2.07	69.97 ± 7.11

879 GS: gastric solid; GL: gastric liquid; IS: intestinal solid; IL: intestinal liquid; G: one-
880 phase homogeneous gastric digest; I: one-phase homogeneous intestinal digest.
881
882 **Table S2.** Gel strength values of agar (A) and κ-carrageenan (KC) hydrogels (HG)
883 formulation with a polysaccharide:protein ratio of 25:75 and 75:25 (coded as 25 and
884 75, respectively).

Sample	Gel strength (N)
HG-A25	$0.59^{b} \pm 0.06$
HG-A75	$4.32^{a} \pm 0.20$
HG-KC25	$0.79^{b} \pm 0.06$
HG-KC75	$4.54^{a} \pm 0.61$

885 Values with different letters are significantly different ($p \leq 0.05$).
886

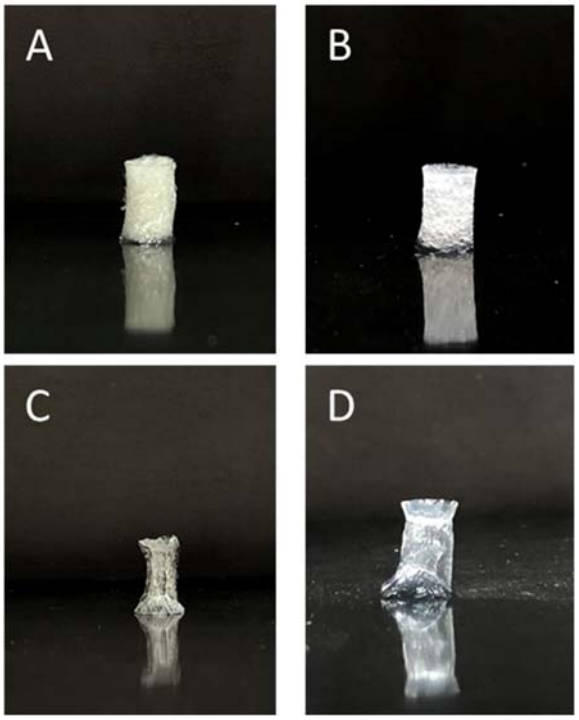

Figure S1. Visual appearance of the pure polysaccharide aerogels from agar (A) and κ-carrageenan (C) and the corresponding solid phases obtained after rehydration in SGF (agar (B), κ-carrageenan (D)).

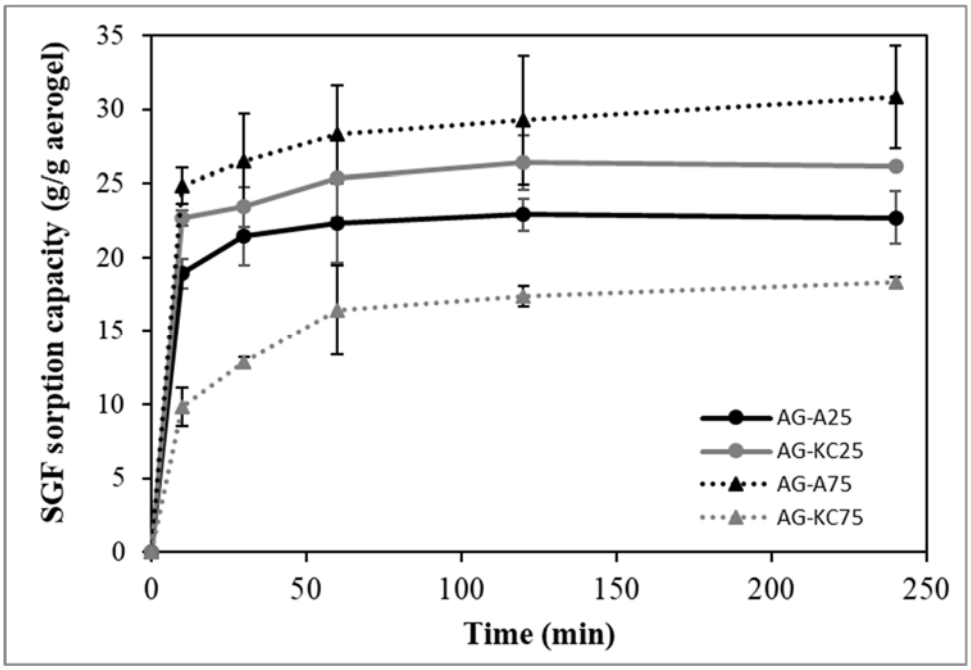

Figure S2. SGF sorption kinetics of the polysaccharide-casein aerogels (AG) formulation with a polysaccharide:protein ratio of 25:75 and 75:25 (coded as 25 and 75, respectively).

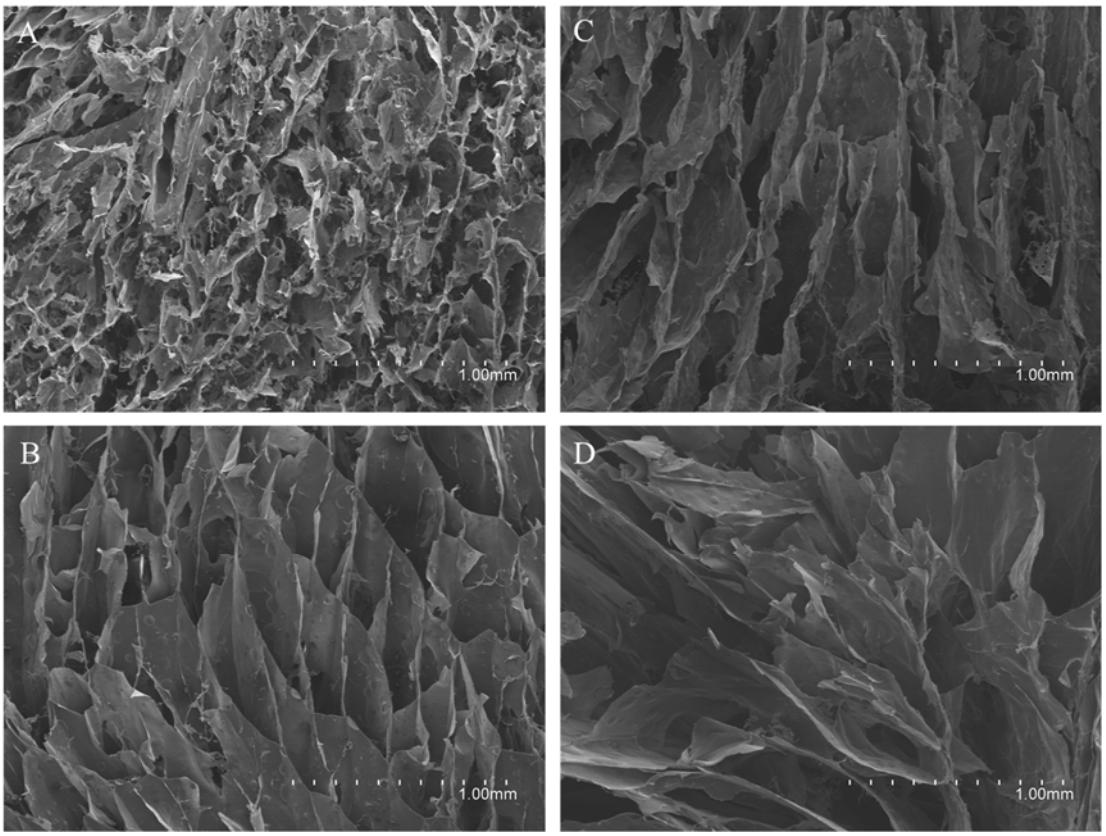

Figure S3. SEM micrographs of the surface from the polysaccharide-casein aerogels. (A) AG-A25, (B) AG-A75, (C) AG-KC25 and (D) AG-KC75. AG refers to aerogel structures and formulations with a polysaccharide:protein ratio of 25:75 and 75:25 are coded as 25 and 75, respectively.

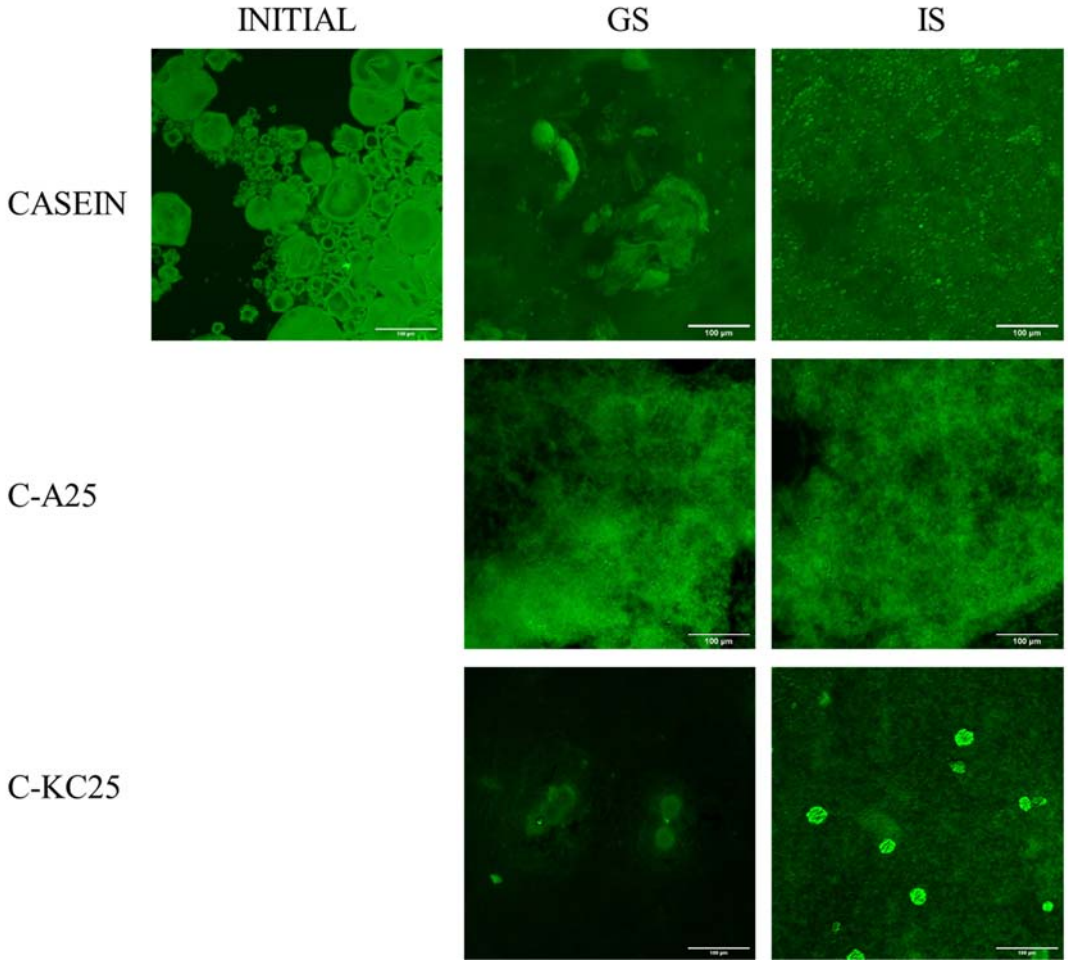

904

905 **Figure S4.** Confocal laser microscopy images of the casein and the control agar- (C-

906 A) and κ carrageenan-casein (C-KC) blends with a polysaccharide:protein ratio of

907 25:75 after the gastric (GS) and intestinal digestions (IS).

908

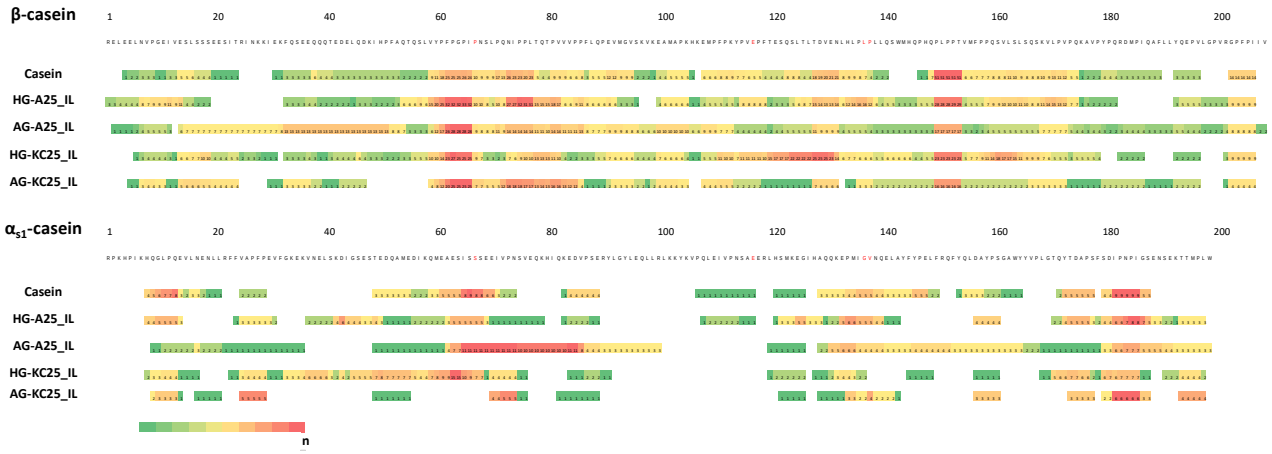

909

Figure S5. Peptide patterns from β-casein, α_{s1}-casein identified in the liquid phase from the intestinal digests (IL) of control casein and the polysaccharide-protein hydrogel (HG) and aerogel (AG) structures with a polysaccharide:protein ratio of 25:75. The colour coding ranges from red (representing the highest number of identified amino acids within a peptide of the corresponding protein) to yellow and green (representing the intermediate to lowest numbers of identified amino acids). White regions represent amino acids without identification within any peptide.